Structural Engineering and Mechanics, *Vol. 71, No. 3 (2019) 257-269*
DOI: https://doi.org/10.12989/sem.2019.71.3.257

Mechanics of nonlocal advanced magneto-electro-viscoelastic plates

Farzad Ebrahimi[1*], Mohammad Reza Barati[1] and Francesco Tornabene[2]

[1]*Mechanical Engineering department, faculty of engineering, Imam Khomeini International University, Qazvin, Iran P.O.B. 34149-16818*
[2]*Department of Civil, Chemical, Environmental, and Materials Engineering, University of Bologna, Bologna, Italy*

(Received May 25, 2018, Revised March 18, 2019, Accepted April 2, 2019)

Abstract. This paper develops a nonlocal strain gradient plate model for damping vibration analysis of smart magneto-electro-viscoelastic nanoplates resting on visco-Pasternak medium. For more accurate analysis of nanoplate, the proposed theory contains two scale parameters related to the nonlocal and strain gradient effects. Viscoelastic effect which is neglected in all previous papers on magneto-electro-viscoelastic nanoplates is considered based on Kelvin–Voigt model. Governing equations of a nonlocal strain gradient smart nanoplate on viscoelastic substrate are derived via Hamilton's principle. Galerkin's method is implemented to solve the governing equations. Effects of different factors such as viscoelasticity, nonlocal parameter, length scale parameter, applied voltage and magnetic potential on damping vibration characteristics of a nanoplate are studied.

Keywords: magneto-electro-viscoelastic nanoplate; free vibration; classical plate theory; nonlocal strain gradient

1. Introduction

Due to having intrinsic coupling effects and adaptive properties, smart structural elements such as beams and plates constructed from the intelligent materials play a major role in different fields of science. The magneto-electro-elastic (MEE) materials are a class of new smart materials which have attracted intense attention of investigators in recent years. Since these materials consist of both piezoelectric and piezomagnetic phases, their mechanical properties can be influenced by exerting magnetic and electric potentials. In the other words, they can exhibit coupling effects between magnetic, electric and thermo-mechanical fields. Analysis of scale-free plates has been performed widely in the literature employing classical theories. But, such theories are not able to examine the scale effects on the nanostructures with small size (Ebrahimi and Salari 2015). Therefore, the nonlocal elasticity theory of Eringen (Eringen and Edelen 1972, Eringen 1983) is developed taking into account small scale effects. Contrary to the local theory in which the stress state at any given point depends only on the strain state at that point, in the nonlocal theory, the stress state at a given point depends on the strain states at all points. The nonlocal elasticity theory has been broadly applied to investigate the mechanical behavior of nanoscale structures (Ebrahimi and Barati 2016a, b, c, d, e, f)

Pradhan and Murmu (2009) examined nonlocal influences on buckling behavior of a single-layer nanoplate subjected to uniform in-plane loadings. Also, Pradhan and Kumar (2011) performed vibration study of orthotropic nanoplates incorporating nonlocal effects using a semi-analytical approach. Application of Levy type method in stability and vibrational investigation of nanosize plates including nonlocal effects is examined by Aksencer and Aydogdu (2011). Mohammadi *et al*. (2014) performed shear buckling analysis of orthotropic nanoplates on elastic substrate including thermal loading effect. In another work, Mohammadi *et al*. (2013) examined the effect of in-plane loading on nonlocal vibrational behavior of circular nanoplates. Also, Ansari *et al*. (2011) explored vibration response of embedded nonlocal multi-layered nanoplates accounting for various boundary conditions. Shen *et al*. (2012) studied vibration behavior of nanomechanical mass sensor based on nonlocal nanoplate model. They showed that vibration response of nanoplates is significantly influenced by the mass of attached nanoparticle. Farajpour *et al*. (2012) examined static stability of nonlocal plates subjected to non-uniform in-plane edge loads. Also, Ansari and Sahmani (2013) employed molecular dynamics simulations to examine biaxial buckling behavior of single-layered graphene sheets based on nonlocal elasticity theory. They matched the results obtained by molecular dynamics simulations with those of nonlocal plate model to extract the appropriate values of nonlocal parameter. Murmu *et al*. (2013) explored the influence of unidirectional magnetic fields on vibrational behavior of nonlocal single-layer graphene sheets resting on elastic substrate. Bessaim *et al*. (2015) presented a nonlocal quasi-3D trigonometric plate model for free vibration behavior of micro/nanoscale plates. Hashemi *et al*. (2015) studied free vibrational behavior of double viscoelastic graphene sheets coupled by visco-Pasternak medium. Arani *et al*. (2016) examined nonlocal vibration of axially moving graphene sheet resting on orthotropic visco-Pasternak foundation under longitudinal magnetic field. Also, Zenkour (2016) performed transient thermal analysis of graphene sheets on viscoelastic foundation based on nonlocal elasticity theory. Ke *et al*. (2015) examined free vibrational response of nonlocal piezoelectric nanoplates considering different boundary

*Corresponding author, Professor
E-mail: febrahimy@eng.ikiu.ac.ir

ISSN: 1225-4568 (Print), 1598-6217 (Online)

conditions. Also, Li *et al*. (2014) investigated stability and vibrational behavior of magneto-electro-elastic nanoplate according to the nonlocal theory. Farajpour *et al*. (2016) presented a nonlocal plate model for nonlinear vibration investigation of magneto-electro-elastic nanoplates. However, effect of viscoelasticity is neglected in these works. Most recently, Ansari and Gholami (2016) explored nonlocal vibrational response of buckled magneto-electro-thermo-elastic nanoplates considering different boundary conditions.

It is clear that all of previous papers on nanoplates applied only the nonlocal elasticity theory to capture small scale effects. However, nonlocal elasticity theory has some limitations in accurate prediction of mechanical behavior of nanostructures. Because, nonlocal elasticity theory is unable to examine the stiffness increment observed in experimental works and strain gradient elasticity (Lam *et al*. 2003). Recently, Lim *et al*. (2015) proposed the nonlocal strain gradient theory to introduce both of the length scales into a single theory. The nonlocal strain gradient theory captures the true influence of the two length scale parameters on the physical and mechanical behavior of small size structures (Li and Hu, Li *et al*. 2016). Recently, Ebrahimi and Barati (2016g, e, 2017a, b) applied the nonlocal strain gradient theory in analysis of nanobeams. They mentioned that mechanical characteristics of nanostructures are significantly affected by stiffness-softening and stiffness-hardening mechanisms due to the nonlocal and strain gradient effects, respectively. Most recently, Ebrahimi *et al*. (Ebrahimi *et al*. 2016) extended the nonlocal strain gradient theory for analysis of nanoplates to obtain the wave frequencies for a range of two scale parameters. So, it is crucial to incorporate both nonlocal and strain gradient effects in analysis of graphene sheets for the first time.

Based on newly developed nonlocal strain gradient theory, damping vibration behavior of smart magneto-electro-viscoelastic nanoplates resting on viscoelastic medium is examined. The theory introduces two scale parameters corresponding to nonlocal and strain gradient effects to capture both stiffness-softening and stiffness-hardening influences. Hamilton's principle is employed to obtain the governing equation of a nonlocal strain gradient nanoplate. These equations are solved via Galerkin's method to obtain the natural frequencies. It is shown that damping vibration behavior of nanoplates is significantly influenced by nonlocal parameter, length scale parameter, viscoelasticity, applied voltage and magnetic potential.

2. Theoretical formulations

The classical plate theory has the following displacement field as:

$$u_1\left(x,y,z,t\right)=u\left(x,y,t\right)-z\frac{\partial w}{\partial x} \tag{1}$$

$$u_2\left(x,y,z,t\right)=v\left(x,y,t\right)-z\frac{\partial w}{\partial y} \tag{2}$$

$$u_3(x,y,z,t)=w(x,y,t) \tag{3}$$

in which $\boldsymbol{u}$ and $\boldsymbol{v}$ are displacement of mid-plane along x, y-axis and w is the bending component of transverse displacement. The electric potential and magnetic potential distributions across the thickness are approximated via a combination of a cosine and linear variation to satisfy Maxwell's equation in the quasi-static approximation as follows:

$$\Phi(x,y,z,t)=-\cos(\xi z)\phi(x,y,t)+\frac{2z}{h}V \tag{4}$$

$$\Upsilon(x,y,z,t)=-\cos(\xi z)\gamma(x,y,t)+\frac{2z}{h}\Omega \tag{5}$$

where $\zeta = \pi / h$. Also, $\boldsymbol{V}$ and Ω are the external electric voltage and magnetic potential applied to the nanoplate. Nonzero strains of the present plate model are expressed by:

$$\begin{Bmatrix}\varepsilon_x\\ \varepsilon_y\\ \gamma_{xy}\end{Bmatrix}=\begin{Bmatrix}\frac{\partial u}{\partial x}\\ \frac{\partial v}{\partial y}\\ \frac{\partial u}{\partial y}+\frac{\partial v}{\partial x}\end{Bmatrix}+z\begin{Bmatrix}-\frac{\partial^2 w}{\partial x^2}\\ -\frac{\partial^2 w}{\partial y^2}\\ -2\frac{\partial^2 w}{\partial x\partial y}\end{Bmatrix} \tag{6}$$

According to Eq. (4), the relation between electric field (E_x, E_y, E_z) and electric potential (Φ), can be obtained as:

$$E_x=-\Phi_{,x}=\cos(\xi z)\frac{\partial\phi}{\partial x}, \tag{7}$$

$$E_y=-\Phi_{,y}=\cos(\xi z)\frac{\partial\phi}{\partial y}, \tag{8}$$

$$E_z=-\Phi_{,z}=-\xi\sin(\xi z)\phi-\frac{2V}{h} \tag{9}$$

Also, the relation between magnetic field (H_x, H_y, H_z) and magnetic potential (Υ) can be expressed from Eq. (5) as:

$$H_x=-\Upsilon_{,x}=\cos(\xi z)\frac{\partial\gamma}{\partial x}, \tag{10}$$

$$H_y=-\Upsilon_{,y}=\cos(\xi z)\frac{\partial\gamma}{\partial y}, \tag{11}$$

$$H_z=-\Upsilon_{,z}=-\xi\sin(\xi z)\gamma-\frac{2\Omega}{h} \tag{12}$$

Through extended Hamilton's principle, the equation of motion can be derived by:

$$\int_0^t\delta(\Pi_S-\Pi_K+\Pi_W)dt=0 \tag{13}$$

Here $\prod_S$ is strain energy, $\prod_W$ is work done by external forces and $\prod_K$ is kinetic energy. The virtual variation of strain energy can be written as:

$$\begin{aligned}&\delta\Pi_S\\&=\int_v\sigma_{ij}\delta\varepsilon_{ij}\,dV\\&=\int_v(\sigma_x\delta\varepsilon_x+\sigma_y\delta\varepsilon_y+\sigma_{xy}\delta\gamma_{xy}+\sigma_{yz}\delta\gamma_{yz}+\sigma_{xz}\delta\gamma_{xz}\\&-D_x\delta E_x-D_y\delta E_y-D_z\delta E_z-B_x\delta H_x-B_y\delta H_y-B_z\delta H_z)dV\end{aligned}\tag{14}$$

Substituting Eq. (6) into Eq. (14) yields:

$$\begin{aligned}&\delta\Pi_S=\int_0^b\int_0^a[N_x\frac{\partial\delta u}{\partial x}-M_x\frac{\partial^2\delta w}{\partial x^2}+N_y\frac{\partial\delta v}{\partial y}\\&-M_y\frac{\partial^2\delta w}{\partial y^2}+N_{xy}(\frac{\partial\delta u}{\partial y}+\frac{\partial\delta v}{\partial x})-2M_{xy}\frac{\partial^2\delta w}{\partial x\partial y}]dxdy\\&+\int_0^b\int_{-h/2}^{h/2}[-D_x\cos(\xi z)\delta\left(\frac{\partial\phi}{\partial x}\right)\\&-D_y\cos(\xi z)\delta\left(\frac{\partial\phi}{\partial y}\right)+D_z\xi\sin(\xi z\delta\phi\\&-B_x\cos(\xi z)\delta\left(\frac{\partial\gamma}{\partial x}\right)-B_y\cos(\xi z\delta\left(\frac{\partial\gamma}{\partial y}\right)\\&+B_z\xi\sin(\xi z)\delta\gamma]dzdxdy\end{aligned}\tag{15}$$

in which the variables at the last expression are expressed by:

$$(N_i,M_i)=\int_A(1,z)\sigma_i\,dA,\ i=(x,y,xy)\tag{16}$$

The variation of the work done by applied loads can be written as:

$$\begin{aligned}&\delta\Pi_W=\int_0^b\int_0^a(N_x^0\frac{\partial w}{\partial x}\frac{\partial\delta w}{\partial x}+N_y^0\frac{\partial w}{\partial y}\frac{\partial\delta w}{\partial y}\\&+2\delta N_{xy}^0\frac{\partial w}{\partial x}\frac{\partial w}{\partial y}-k_w\delta w-c_d\delta\frac{\partial w}{\partial t}\\&+k_p(\frac{\partial w}{\partial x}\frac{\partial\delta w}{\partial x}+\frac{\partial w}{\partial y}\frac{\partial\delta w}{\partial y}))dxdy\end{aligned}\tag{17}$$

where N_x^0, N_y^0, N_{xy}^0 are in-plane applied loads; k_w, k_p and c_d are Winkler, Pasternak and damping constants. The variation of the kinetic energy is calculated as:

$$\begin{aligned}&\delta K=\int_0^b\int_0^a[I_0(\frac{\partial u}{\partial t}\frac{\partial\delta u}{\partial t}+\frac{\partial v}{\partial t}\frac{\partial\delta v}{\partial t}+\frac{\partial w}{\partial t}\frac{\partial\delta w}{\partial t})\\&-I_1(\frac{\partial u}{\partial t}\frac{\partial\delta w}{\partial x\partial t}+\frac{\partial w}{\partial x\partial t}\frac{\partial\delta u}{\partial t}+\frac{\partial v}{\partial t}\frac{\partial\delta w}{\partial y\partial t}\\&+\frac{\partial w}{\partial y\partial t}\frac{\partial\delta v}{\partial t})+I_2(\frac{\partial w}{\partial x\partial t}\frac{\partial\delta w}{\partial x\partial t}+\frac{\partial w}{\partial y\partial t}\frac{\partial\delta w}{\partial y\partial t})]dxdy\end{aligned}\tag{18}$$

in which:

$$(I_0,I_2)=\int_{-h/2}^{h/2}(1,z^2)\rho dz,I_1=\int_{-h/2}^{h/2}\rho zdz=0\tag{19}$$

The following Euler–Lagrange equations are obtained by inserting Eqs. (14)-(18) in Eq. (13) when the coefficients of δu, δv, δw, $\delta\phi$ and $\delta\gamma$ are equal to zero:

$$\frac{\partial N_x}{\partial x}+\frac{\partial N_{xy}}{\partial y}=I_0\frac{\partial^2 u}{\partial t^2}\tag{20}$$

$$\frac{\partial N_{xy}}{\partial x}+\frac{\partial N_y}{\partial y}=I_0\frac{\partial^2 v}{\partial t^2}\tag{21}$$

$$\begin{aligned}&\frac{\partial^2 M_x}{\partial x^2}+2\frac{\partial^2 M_{xy}}{\partial x\partial y}+\frac{\partial^2 M_y}{\partial y^2}-(N^E+N^H-k_p)\nabla^2 w\\&-k_w w-c_d\frac{\partial w}{\partial t}=I_0\frac{\partial^2 w}{\partial t^2}-I_2\nabla^2(\frac{\partial^2 w}{\partial t^2})\end{aligned}\tag{22}$$

$$\int_{-h/2}^{h/2}\left(\cos(\xi z)\frac{\partial D_x}{\partial x}+\cos(\xi z)\frac{\partial D_y}{\partial y}+\xi\sin(\xi z)D_z\right)dz=0\tag{23}$$

$$\int_{-h/2}^{h/2}\left(\cos(\xi z)\frac{\partial B_x}{\partial x}+\cos(\xi z)\frac{\partial B_y}{\partial y}+\xi\sin(\xi z)B_z\right)dz=0\tag{24}$$

2.1 Nonlocal strain gradient theory for the magneto-electro-elastic materials

The newly developed nonlocal strain gradient theory (Ebrahimi *et al*. 2016) takes into account both nonlocal stress field and the strain gradient effects by introducing two scale parameters. This theory defines the stress field as:

$$\sigma_{ij}=\sigma_{ij}^{(0)}-\frac{d\sigma_{ij}^{(1)}}{dx}\tag{25}$$

in which the stresses $\sigma_{xx}^{(0)}$ and $\sigma_{xx}^{(1)}$ are corresponding to strain ε_{xx} and strain gradient $\varepsilon_{xx,x}$, respectively as:

$$\sigma_{ij}^{(0)}=\int_0^L C_{ijkl}\alpha_0(x,x',e_0a)\varepsilon'_{kl}(x')dx'\tag{26}$$

$$\sigma_{ij}^{(1)}=l^2\int_0^L C_{ijkl}\alpha_1(x,x',e_1a)\varepsilon'_{kl,x}(x')dx'\tag{27}$$

in which C_{ijkl} are the elastic coefficients and e_0a and e_1a capture the nonlocal effects and l captures the strain gradient effects. When the nonlocal functions $\alpha_0(x, x', e_0a)$ and $\alpha_1(x, x', e_1a)$ satisfy the developed conditions by Eringen (Eringen 1983), the constitutive relation of nonlocal strain gradient theory has the following form:

$$\begin{aligned}&[1-(e_1a)^2\nabla^2][1-(e_0a)^2\nabla^2]\sigma_{ij}\\&=C_{ijkl}[1-(e_1a)^2\nabla^2]\varepsilon_{kl}-C_{ijkl}\,l^2[1-(e_0a)^2\nabla^2]\nabla^2\varepsilon_{kl}\end{aligned}\tag{28}$$

in which ∇^2 denotes the Laplacian operator. Considering $e_1 = e_0 = e$, the general constitutive relation in Eq. (22a) becomes

$$[1-(ea)^2\nabla^2]\sigma_{ij}=C_{ijkl}[1-l^2\nabla^2]\varepsilon_{kl}\tag{29}$$

The nonlocal strain gradient theory can be extended for the

MEE nanoplates as:

$$\sigma_{ij}-(ea)^2\nabla^2\sigma_{ij}=(1-l^2\nabla^2)[C_{ijkl}\varepsilon_{kl}-e_{mij}E_m-q_{nij}H_n] \quad (30a)$$

$$D_i-(ea)^2\nabla^2 D_i=(1-l^2\nabla^2)[e_{ikl}\varepsilon_{kl}+s_{im}E_m+d_{in}H_n] \quad (30b)$$

$$B_i-(ea)^2\nabla^2 B_i=(1-l^2\nabla^2)[q_{ikl}\varepsilon_{kl}+d_{im}E_m+\chi_{in}H_n] \quad (30c)$$

where ∇^2 is the Laplacian operator. The stress-strain relations can be expressed by:

$$\begin{aligned}&(1-\mu\nabla^2)\sigma_{xx}\\&=(1-\lambda\nabla^2)[\tilde{c}_{11}\varepsilon_{xx}+\tilde{c}_{12}\varepsilon_{yy}-\tilde{e}_{31}E_z-\tilde{q}_{31}H_z]\end{aligned} \quad (31)$$

$$\begin{aligned}&(1-\mu\nabla^2)\sigma_{yy}\\&=(1-\lambda\nabla^2)[\tilde{c}_{12}\varepsilon_{xx}+\tilde{c}_{22}\varepsilon_{yy}-\tilde{e}_{32}E_z-\tilde{q}_{32}H_z]\end{aligned} \quad (32)$$

$$(1-\mu\nabla^2)\sigma_{xy}=(1-\lambda\nabla^2)\tilde{c}_{66}\gamma_{xy} \quad (33)$$

$$(1-\mu\nabla^2)D_x=(1-\lambda\nabla^2)[\tilde{k}_{11}E_x+\tilde{d}_{11}H_x] \quad (34)$$

$$(1-\mu\nabla^2)D_y=(1-\lambda\nabla^2)[\tilde{k}_{11}E_y+\tilde{d}_{11}H_y] \quad (35)$$

$$\begin{aligned}&(1-\mu\nabla^2)D_z\\&=(1-\lambda\nabla^2)[\tilde{e}_{31}\varepsilon_{xx}+\tilde{e}_{31}\varepsilon_{yy}+\tilde{k}_{33}E_z+\tilde{d}_{33}H_z]\end{aligned} \quad (36)$$

$$(1-\mu\nabla^2)B_x=(1-\lambda\nabla^2)[\tilde{q}_{15}\gamma_{xz}+\tilde{d}_{11}E_x+\tilde{\chi}_{11}H_x] \quad (37)$$

$$(1-\mu\nabla^2)B_y=(1-\lambda\nabla^2)[\tilde{q}_{15}\gamma_{yz}+\tilde{d}_{11}E_y+\tilde{\chi}_{11}H_y] \quad (38)$$

$$\begin{aligned}&(1-\mu\nabla^2)B_z\\&=(1-\lambda\nabla^2)[\tilde{q}_{31}\varepsilon_{xx}+\tilde{q}_{31}\varepsilon_{yy}+\tilde{d}_{33}E_z+\tilde{\chi}_{33}H_z]\end{aligned} \quad (39)$$

where $\mu = (ea)^2$ and $\lambda = l^2$. Also, $\tilde{c}_{ij}, \tilde{e}_{ij}, \tilde{q}_{ij}, \tilde{d}_{ij}, \tilde{s}_{ij}$ and $\tilde{\chi}_{ij}$ are reduced constants for the plate under the plane stress state which are given as

$$\begin{aligned}&\tilde{c}_{11}=c_{11}-\frac{c_{13}^2}{c_{33}},\ \tilde{c}_{12}=c_{12}-\frac{c_{13}^2}{c_{33}},\\&\tilde{c}_{66}=c_{66},\quad \tilde{e}_{15}=e_{15},\quad \tilde{e}_{31}=e_{31}-\frac{c_{13}e_{33}}{c_{33}},\\&\tilde{q}_{15}=q_{15},\ \tilde{q}_{31}=q_{31}-\frac{c_{13}q_{33}}{c_{33}},\\&\tilde{d}_{11}=\tilde{d}_{11},\quad \tilde{d}_{33}=\tilde{d}_{33}+\frac{q_{33}e_{33}}{c_{33}},\\&\tilde{k}_{11}=k_{11},\quad \tilde{k}_{33}=k_{33}+\frac{e_{33}^2}{c_{33}},\\&\tilde{\chi}_{11}=\chi_{11},\quad \tilde{\chi}_{33}=\chi_{33}+\frac{q_{33}^2}{c_{33}}\end{aligned} \quad (40)$$

Inserting Eqs. (31)-(39) in Eq. (16) and considering Kelvin-Voigt viscoelastic model gives:

$$\begin{aligned}&(1-\mu\nabla^2)\begin{Bmatrix}N_x\\N_y\\N_{xy}\end{Bmatrix}\\&=(1-\lambda\nabla^2)[(1+g\frac{\partial}{\partial t})\begin{pmatrix}A_{11}&A_{12}&0\\A_{12}&A_{22}&0\\0&0&A_{66}\end{pmatrix}\begin{Bmatrix}\frac{\partial u}{\partial x}\\\frac{\partial v}{\partial y}\\\frac{\partial u}{\partial y}+\frac{\partial v}{\partial x}\end{Bmatrix}\\&+(1+g\frac{\partial}{\partial t})\begin{pmatrix}B_{11}&B_{12}&0\\B_{12}&B_{22}&0\\0&0&B_{66}\end{pmatrix}\begin{Bmatrix}-\frac{\partial^2 w}{\partial x^2}\\-\frac{\partial^2 w}{\partial y^2}\\-2\frac{\partial^2 w}{\partial x\partial y}\end{Bmatrix}\\&+\begin{Bmatrix}A_{31}^e\\A_{31}^e\\0\end{Bmatrix}\phi+\begin{Bmatrix}A_{31}^m\\A_{31}^m\\0\end{Bmatrix}\gamma]-\begin{Bmatrix}N_x^E\\N_y^E\\0\end{Bmatrix}-\begin{Bmatrix}N_x^H\\N_y^H\\0\end{Bmatrix}\end{aligned} \quad (41)$$

$$\begin{aligned}&(1-\mu\nabla^2)\begin{Bmatrix}M_x\\M_y\\M_{xy}\end{Bmatrix}\\&=(1-\lambda\nabla^2)[(1+g\frac{\partial}{\partial t})\begin{pmatrix}B_{11}&B_{12}&0\\B_{12}&B_{22}&0\\0&0&B_{66}\end{pmatrix}\begin{Bmatrix}\frac{\partial u}{\partial x}\\\frac{\partial v}{\partial y}\\\frac{\partial u}{\partial y}+\frac{\partial v}{\partial x}\end{Bmatrix}\\&+(1+g\frac{\partial}{\partial t})\begin{pmatrix}D_{11}&D_{12}&0\\D_{12}&D_{22}&0\\0&0&D_{66}\end{pmatrix}\begin{Bmatrix}-\frac{\partial^2 w}{\partial x^2}\\-\frac{\partial^2 w}{\partial y^2}\\-2\frac{\partial^2 w}{\partial x\partial y}\end{Bmatrix}\\&+\begin{Bmatrix}E_{31}^e\\E_{31}^e\\0\end{Bmatrix}\phi+\begin{Bmatrix}E_{31}^m\\E_{31}^m\\0\end{Bmatrix}\gamma]-\begin{Bmatrix}M_x^E\\M_y^E\\0\end{Bmatrix}-\begin{Bmatrix}M_x^H\\M_y^H\\0\end{Bmatrix}\end{aligned} \quad (42)$$

$$\begin{aligned}\int_{-h/2}^{h/2}(1-\mu\nabla^2)\begin{Bmatrix}D_x\\D_y\end{Bmatrix}\cos(\xi z)\,dz=(1-\lambda\nabla^2)[F_{11}^e\begin{Bmatrix}\frac{\partial\phi}{\partial x}\\\frac{\partial\phi}{\partial y}\end{Bmatrix}\\+F_{11}^m\begin{Bmatrix}\frac{\partial\gamma}{\partial x}\\\frac{\partial\gamma}{\partial y}\end{Bmatrix}]\end{aligned} \quad (43)$$

$$(1-\mu\nabla^2)\int_{-h/2}^{h/2} D_z\xi\sin(\xi z)\,dz = (1-\lambda\nabla^2)[A_{31}^e\left(\frac{\partial u}{\partial x}+\frac{\partial v}{\partial y}\right) - E_{31}^e\nabla^2 w - F_{33}^e\phi - F_{33}^m\gamma] \tag{44}$$

$$\int_{-h/2}^{h/2}(1-\mu\nabla^2)\begin{Bmatrix}B_x\\B_y\end{Bmatrix}\cos(\xi z)\,dz = (1-\lambda\nabla^2)[F_{11}^m\begin{Bmatrix}\frac{\partial\phi}{\partial x}\\\frac{\partial\phi}{\partial y}\end{Bmatrix} + X_{11}^m\begin{Bmatrix}\frac{\partial\gamma}{\partial x}\\\frac{\partial\gamma}{\partial y}\end{Bmatrix}] \tag{45}$$

$$\int_{-h/2}^{h/2}(1-\mu\nabla^2)B_z\xi\,\sin(\xi z)\,dz = (1-\lambda\nabla^2)[A_{31}^m\left(\frac{\partial u}{\partial x}+\frac{\partial v}{\partial y}\right) - E_{31}^m\nabla^2 w - F_{33}^m\phi - X_{33}^m\gamma] \tag{46}$$

in which

$$\begin{Bmatrix}A_{11},D_{11}\\A_{12},D_{12}\\A_{66},D_{66}\end{Bmatrix} = \int_{-h/2}^{h/2}\begin{Bmatrix}\tilde{c}_{11}\\\tilde{c}_{12}\\\tilde{c}_{66}\end{Bmatrix}(1,z^2)dz \tag{47}$$

$$\left\{A_{31}^e,E_{31}^e\right\} = \int_{-h/2}^{h/2}\tilde{e}_{31}\xi\sin(\xi z)\left\{1,z\right\}dz \tag{48}$$

$$\left\{A_{31}^m,E_{31}^m\right\} = \int_{-h/2}^{h/2}\tilde{q}_{31}\xi\sin(\xi z)\left\{1,z\right\}dz \tag{49}$$

$$\left\{F_{11}^e,F_{33}^e\right\} = \int_{-h/2}^{h/2}\left\{\tilde{k}_{11}\cos^2(\xi z),\tilde{k}_{33}\,\xi^2\sin^2(\xi z)\right\}dz \tag{50}$$

$$\left\{F_{11}^m,F_{33}^m\right\} = \int_{-h/2}^{h/2}\left\{\tilde{d}_{11}\cos^2(\xi z),\tilde{d}_{33}\,\xi^2\sin^2(\xi z)\right\}dz \tag{51}$$

$$\left\{X_{11}^m,X_{33}^m\right\} = \int_{-h/2}^{h/2}\left\{\tilde{\chi}_{11}\cos^2(\xi z),\tilde{\chi}_{33}\,\xi^2\sin^2(\xi z)\right\}dz \tag{52}$$

Also, normal forces and moments due to magneto-electrical field in Eqs. (40) and (41) can be defined by:

$$\begin{aligned}N_x^E &= N_y^E = -\int_{-h/2}^{h/2}\tilde{e}_{31}\frac{2V}{h}dz,\\ N_x^H &= N_y^H = -\int_{-h/2}^{h/2}\tilde{q}_{31}\frac{2\Omega}{h}dz\end{aligned} \tag{53a}$$

$$\begin{aligned}M_x^E &= M_y^E = -\int_{-h/2}^{h/2}\tilde{e}_{31}\frac{2V}{h}zdz,\\ M_x^H &= M_y^H = -\int_{-h/2}^{h/2}\tilde{q}_{31}\frac{2\Omega}{h}zdz\end{aligned} \tag{53b}$$

The governing equations of nonlocal strain gradient nanoplate under magneto-electrical coupling in terms of the displacement can be derived by substituting Eqs. (41)-(46), into Eqs. (20) -(24) as follows:

$$\begin{aligned}&(1-\lambda\nabla^2)[(1+g\frac{\partial}{\partial t})A_{11}\frac{\partial^2 u}{\partial x^2}+(1+g\frac{\partial}{\partial t})A_{66}\frac{\partial^2 u}{\partial y^2}\\&+(1+g\frac{\partial}{\partial t})(A_{12}+A_{66})\frac{\partial^2 v}{\partial x\partial y}-(1+g\frac{\partial}{\partial t})B_{11}\frac{\partial^3 w}{\partial x^3}\\&-(1+g\frac{\partial}{\partial t})(B_{12}+2B_{66})\frac{\partial^3 w}{\partial x\partial y^2}+A_{31}^e\frac{\partial\phi}{\partial x}+A_{31}^m\frac{\partial\gamma}{\partial x}]\\&+(1-\mu\nabla^2)(-I_0\frac{\partial^2 u}{\partial t^2}+I_1\frac{\partial^3 w}{\partial x\partial t^2})=0\end{aligned} \tag{54}$$

$$\begin{aligned}&(1-\lambda\nabla^2)[(1+g\frac{\partial}{\partial t})A_{66}\frac{\partial^2 v}{\partial x^2}+(1+g\frac{\partial}{\partial t})A_{22}\frac{\partial^2 v}{\partial y^2}\\&+(1+g\frac{\partial}{\partial t})(A_{12}+A_{66})\frac{\partial^2 u}{\partial x\partial y}-(1+g\frac{\partial}{\partial t})B_{22}\frac{\partial^3 w}{\partial y^3}\\&-(1+g\frac{\partial}{\partial t})(B_{12}+2B_{66})\frac{\partial^3 w}{\partial x^2\partial y}+A_{31}^e\frac{\partial\phi}{\partial y}\\&+A_{31}^m\frac{\partial\gamma}{\partial y}]+(1-\mu\nabla^2)(-I_0\frac{\partial^2 v}{\partial t^2}+I_1\frac{\partial^3 w}{\partial y\partial t^2})=0\end{aligned} \tag{55}$$

$$\begin{aligned}&(1-\lambda\nabla^2)[(1+g\frac{\partial}{\partial t})B_{11}\frac{\partial^3 u}{\partial x^3}+(1+g\frac{\partial}{\partial t})(B_{12}+2B_{66})\frac{\partial^3 u}{\partial x\partial y^2}\\&+(1+g\frac{\partial}{\partial t})(B_{12}+2B_{66})\frac{\partial^3 v}{\partial x^2\partial y}+(1+g\frac{\partial}{\partial t})B_{22}\frac{\partial^3 v}{\partial y^3}\\&-(1+g\frac{\partial}{\partial t})D_{11}\frac{\partial^4 w}{\partial x^4}+E_{31}^e(\frac{\partial^2\phi}{\partial x^2}+\frac{\partial^2\phi}{\partial y^2})\\&-2(1+g\frac{\partial}{\partial t})(D_{12}+2D_{66})\frac{\partial^4 w}{\partial x^2\partial y^2}\\&-(1+g\frac{\partial}{\partial t})D_{22}\frac{\partial^4 w}{\partial y^4}+E_{31}^m(\frac{\partial^2\gamma}{\partial x^2}+\frac{\partial^2\gamma}{\partial y^2})]\\&+(1-\mu\nabla^2)(-I_0\frac{\partial^2 w}{\partial t^2}-I_1(\frac{\partial^3 u}{\partial x\partial t^2}+\frac{\partial^3 v}{\partial y\partial t^2})\\&+I_2(\frac{\partial^4 w}{\partial x^2\partial t^2}+\frac{\partial^4 w}{\partial y^2\partial t^2})-(N^E+N^H-k_p)(\frac{\partial^2 w}{\partial x^2}+\frac{\partial^2 w}{\partial y^2})\\&-k_w w-c_d\frac{\partial w}{\partial t})=0\end{aligned} \tag{56}$$

$$\begin{aligned}&(1-\lambda\nabla^2)[A_{31}^e(\frac{\partial u}{\partial x}+\frac{\partial v}{\partial y})-E_{31}^e(\frac{\partial^2 w}{\partial x^2}+\frac{\partial^2 w}{\partial y^2})\\&+F_{11}^e(\frac{\partial^2\phi}{\partial x^2}+\frac{\partial^2\phi}{\partial y^2})+F_{11}^m(\frac{\partial^2\gamma}{\partial x^2}+\frac{\partial^2\gamma}{\partial y^2})\\&-F_{33}^e\phi-F_{33}^m\gamma]=0\end{aligned} \tag{57}$$

$$\begin{aligned}&(1-\lambda\nabla^2)[A_{31}^m(\frac{\partial u}{\partial x}+\frac{\partial v}{\partial y})-E_{31}^m(\frac{\partial^2 w}{\partial x^2}+\frac{\partial^2 w}{\partial y^2})\\&+F_{11}^m(\frac{\partial^2\phi}{\partial x^2}+\frac{\partial^2\phi}{\partial y^2})+X_{11}^m(\frac{\partial^2\gamma}{\partial x^2}+\frac{\partial^2\gamma}{\partial y^2})\\&-F_{33}^m\phi-X_{33}^m\gamma]=0\end{aligned} \tag{58}$$

It is assumed that the nanoplate is exposed to external electric voltage, magnetic potential and the shear loading is ignored. So $N_{xy}^0 = 0$ and N_x^0, N_y^0 are the normal forces induced by external electric voltage V and external magnetic potential Ω, respectively and are defined as

$$N_x^0 = N_y^0 = N^E + N^H$$
$$N^E = -\int_{-h/2}^{h/2} \tilde{e}_{31} \frac{2V}{h} dz, N^H = -\int_{-h/2}^{h/2} \tilde{q}_{31} \frac{2\Omega}{h} dz \tag{59}$$

3. Solution by Galerkin's method

In this section, Galerkin's method is implemented to solve the governing equations of smart nonlocal strain gradient nanoplates. Thus, the displacement field can be calculated as:

$$u = \sum_{m=1}^{\infty}\sum_{n=1}^{\infty} U_{mn} \frac{\partial X_m(x)}{\partial x} Y_n(y) e^{i\omega_n t} \tag{60}$$

$$v = \sum_{m=1}^{\infty}\sum_{n=1}^{\infty} V_{mn} X_m(x) \frac{\partial Y_n(y)}{\partial y} e^{i\omega_n t} \tag{61}$$

$$w = \sum_{m=1}^{\infty}\sum_{n=1}^{\infty} W_{mn} X_m(x) Y_n(y) e^{i\omega_n t} \tag{62}$$

$$\phi = \sum_{m=1}^{\infty}\sum_{n=1}^{\infty} \Phi_{mn} X_m(x) Y_n(y) e^{i\omega_n t} \tag{63}$$

$$\gamma = \sum_{m=1}^{\infty}\sum_{n=1}^{\infty} \Upsilon_{mn} X_m(x) Y_n(y) e^{i\omega_n t} \tag{64}$$

where (U_{mn}, V_{mn}, W_{bmn}, Φ_{mn}, Υ_{mn}) are the unknown coefficients. Inserting Eqs. (60) - (64) into Eqs. (54) -(58) respectively, leads to:

$$\begin{aligned}
&[(1+ig\omega)\big(A_{11}(r_1-\lambda(r_{12}+r_{13})+A_{66}(r_2-\lambda(r_{13}+r_{14})\big)\\
&+I_0\omega^2(r_{11}-\mu(r_2+r_1))]U_{mn}\\
&+(1+ig\omega)\big(A_{12}+A_{66}\big)(r_2-\lambda(r_{13}+r_{14})V_{mn}\\
&-[(1+ig\omega)B_{11}(r_1-\lambda(r_{12}+r_{13})_1\\
&+(1+ig\omega)\big(B_{12}+2B_{66}\big)(r_2-\lambda(r_{13}+r_{14})\\
&+I_1\omega^2 r_{11}-\mu I_1\omega_n^2(r_1+r_2)]W_{bmn}+A_{31}^e r_{11}\Phi_{mn}+A_{31}^m r_{11}\Upsilon_{mn}=0
\end{aligned} \tag{65}$$

$$\begin{aligned}
&[(1+ig\omega)(A_{12}+A_{66})(r_3-\lambda(r_{15}+r_{16}))]U_{mn}\\
&+[(1+ig\omega)A_{66}(r_3-\lambda(r_{15}+r_{16}))\\
&+(1+ig\omega)A_{22}(r_4-\lambda(r_{16}+r_{17}))-I_0\omega_n^2(\mu(r_3+r_4)-r_{12})]V_{mn}\\
&+[-(1+ig\omega)B_{22}(r_4-\lambda(r_{16}+r_{17})\\
&-(1+ig\omega)(B_{12}+2B_{66})(r_3-\lambda(r_{15}+r_{16})\\
&-I_1\omega_n^2(r_{12}-\mu(r_3+r_4))]W_{mn}+A_{31}^e r_{12}\Phi_{mn}+A_{31}^m r_{12}\Upsilon_{mn}=0
\end{aligned} \tag{66}$$

$$\begin{aligned}
&[(1+ig\omega)B_{11}(r_5-\lambda(r_{18}+r_{19}))\\
&+(1+ig\omega)(B_{12}+2B_{66})(r_6-\lambda(r_{18}+r_{20}))\\
&+I_1\omega_n^2(\mu(r_5+r_6)-r_{10})]U_{mn}\\
&+[(1+ig\omega)(B_{12}+2B_{66})(r_6-\lambda(r_{18}+r_{20}))\\
&+(1+ig\omega)B_{22}r_7-I_1\omega_n^2(\mu(r_6+r_7)-r_9)]V_{mn}\\
&+[-(1+ig\omega)D_{11}(r_5-\lambda(r_{18}+r_{19}))_5\\
&-2(1+ig\omega)(D_{12}+2D_{66})(r_6-\lambda(r_{18}+r_{20}))\\
&-(1+ig\omega)D_{22}r_7-I_2\omega_n^2((r_{10}+r_9)\\
&-\mu(2r_6+r_5+r_7))-I_0\omega_n^2(\mu(r_9+r_{10})-r_8)\\
&+(N^E+N^H-k_p)(\mu(r_5+2r_6+r_7)\\
&-(r_{10}+r_9))-(k_w+ic_d\omega)(r_8-\mu(r_9+r_{10}))]W_{mn}\\
&+[E_{31}^e(r_{10}+r_9)]\Phi_{mn}+[E_{31}^m(r_9+r_{10})]\Upsilon_{mn}=0
\end{aligned} \tag{67}$$

$$\begin{aligned}
&A_{31}^e(r_{10}-\lambda(r_5+r_6))U_{mn}+A_{31}^e(r_9-\lambda(r_6+r_7))V_{mn}\\
&+[-E_{31}^e((r_{10}-\lambda(r_5+r_6))+(r_9-\lambda(r_6+r_7)))]W_{mn}\\
&+[F_{11}^e((r_{10}-\lambda(r_5+r_6))+(r_9-\lambda(r_6+r_7)))\\
&-F_{33}^e(r_8-\lambda(r_9+r_{10}))]\Phi_{mn}\\
&+[F_{11}^m((r_{10}-\lambda(r_5+r_6))+(r_9-\lambda(r_6+r_7)))\\
&-F_{33}^m(r_8-\lambda(r_9+r_{10}))]\Upsilon_{mn}=0
\end{aligned} \tag{68}$$

$$\begin{aligned}
&A_{31}^m(r_{10}-\lambda(r_5+r_6))U_{mn}+A_{31}^m(r_9-\lambda(r_6+r_7))V_{mn}\\
&-E_{31}^m((r_{10}-\lambda(r_5+r_6))+(r_9-\lambda(r_6+r_7)))W_{mn}\\
&+[F_{11}^m((r_{10}-\lambda(r_5+r_6))+(r_9-\lambda(r_6+r_7)))\\
&-F_{33}^m(r_8-\lambda(r_9+r_{10}))]\Phi_{mn}\\
&+[X_{11}^m((r_{10}-\lambda(r_5+r_6))+(r_9-\lambda(r_6+r_7)))\\
&-X_{33}^m(r_8-\lambda(r_9+r_{10}))]\Upsilon_{mn}=0
\end{aligned} \tag{69}$$

where

$$\begin{aligned}
&\{r_3, r_4, r_{12}\}\\
&= \int_0^a\int_0^b X(x)Y^{(1)}(y)\{X^{(2)}(x)Y^{(1)}(y), X(x)Y^{(3)}(y),\\
&\qquad X(x)Y^{(1)}(y)\}dxdy
\end{aligned} \tag{70}$$

$$\{r_1, r_2, r_{11}\} = \int_0^a\int_0^b X^{(1)}(x)Y(y)\{X^{(3)}(x)Y(y), X'(x)Y''(y), X'(x)Y(y)\}dxdy \tag{71}$$

$$\{r_5, r_6, r_7\} = \int_0^a\int_0^b X(x)Y(y)\{X^{(4)}(x)Y(y), X^{(2)}(x)Y^{(2)}(y), X(x)Y^{(4)}(y)\}dxdy \tag{72}$$

$$\{r_8, r_9, r_{10}\} = \int_0^a\int_0^b X(x)Y(y)\{X(x)Y(y), X(x)Y^{(2)}(y), X^{(2)}(x)Y(y)\}dxdy \tag{73}$$

$$\begin{aligned}
&\{r_{12}, r_{13}, r_{14}\}\\
&= \int_0^a\int_0^b X^{(1)}(x)Y(y)\{X^{(5)}(x)Y(y), X^{(3)}(x)Y^{(2)}(y),\\
&\qquad X^{(1)}(x)Y^{(4)}(y)\}dxdy
\end{aligned} \tag{74}$$

$$\{r_{15}, r_{16}, r_{17}\} = \int_0^a \int_0^b X(x)Y^{(1)}(y)\{X^{(4)}(x)Y^{(1)}(y), X^{(2)}(x)Y^{(3)}(y), X(x)Y^{(5)}(y)\}dxdy \quad (75)$$

$$\{r_{18}, r_{19}, r_{20}\} = \int_0^a \int_0^b X(x)Y(y)\{X^{(4)}(x)Y^{(2)}(y), X^{(6)}(x)Y(y), X^{(2)}(x)Y^{(4)}(y)\}dxdy \quad (76)$$

The function X for simply-supported boundary conditions is defined by:

$$\text{SS:} \quad \begin{matrix} \mathrm{X}_m(x) = \sin(\lambda_m x) \\ \lambda_m = \dfrac{m\pi}{a} \end{matrix} \quad (77)$$

The function Y can be obtained by replacing x, m and a, respectively by y, n and b. By finding determinant of the coefficient matrix of the following equations and setting this multinomial to zero, we can find vibration frequencies.

$$\left[[K]+\omega[C]+\omega^2[M]\right]\begin{Bmatrix} U_{mn} \\ V_{mn} \\ W_{mn} \\ \Phi_{mn} \\ \Upsilon_{mn} \end{Bmatrix} = 0 \quad (78)$$

In which [K], [C] and [M] are stiffness, damping and mass matrices, respectively. It should be noted that calculations are performed based on the following dimensionless quantities:

$$\hat{\omega} = \omega \frac{\mathrm{a}^2}{h}\sqrt{\frac{\rho}{\mathrm{c}_{11}}}, \quad K_w = \mathrm{k}_w \frac{\mathrm{a}^4}{D^*},$$
$$K_p = \mathrm{k}_p \frac{\mathrm{a}^2}{D^*}, \quad D^* = c_{11}h^3, \quad (79)$$
$$C_d = c_d \frac{a^2}{\sqrt{\rho h D^*}}, G_d = g\frac{h}{\mathrm{a}^2}\sqrt{\frac{c_{11}}{\rho}}$$

4. Numerical results and discussions

This section is devoted to study the damping vibration behavior of nonlocal strain gradient magneto-electro-viscoelastic nanoplates on viscoelastic substrate based on classical plate theory. The model introduces two scale coefficients related to nonlocal and strain gradient effects for more accurate analysis of smart nanoplates. Material properties of the nanoplate are presented in Table 1. Configuration of nanoplate on viscoelastic medium is shown in Fig. 1. The nanoplate geometry has the following dimensions: a (length) = 10 nm and h (thickness) = varied.

Natural frequencies of a piezoelectric nanoplate are validated with those obtained by Ke *et al*. (2015) for various nonlocal parameters (μ=0, 0.1, 0.2, 0.3, 0.4, 0.5). Obtained frequencies via present Galerkin method are in excellent agreement with those of exact solution presented by Ke *et al*. (2015), as tabulated in Table 1. For comparison study, the strain gradient parameter is set to zero (λ=0).

Examination of nonlocal and strain gradient effects on the real and imaginary parts of vibration frequencies with respect to damping coefficient (C_d) is presented in Fig. 2

Table 1 Magneto-electro-elastic coefficients of material properties

Properties	$BaTiO_3 - CoFe_2O_4$
$c_{11} = c_{22}$ (GPa)	266
c_{33}	216
$c_{13} = c_{23}$	124
c_{12}	125
c_{55}	44.2
c_{66}	50.5
e_{31} (Cm^{-2})	-2.2
e_{33}	9.3
e_{15}	5.8
q_{31} (N/Am)	290.1
q_{33}	349.9
q_{15}	275
k_{11} (10^{-9} C^2 m^{-2} N^{-1})	5.64
k_{33}	6.35
χ_{11}(10^{-6} Ns^2C^{-2} /2)	-297
χ_{33}	83.5
$d_{11} = d_{22}$	5.367
d_{33}	2737.5
ρ (kgm^{-3})	5550

Table 2 Comparison of non-dimensional frequency of piezoelectric nanoplates with simply-supported and clamped boundary conditions (V=0)

	Nonlocal parameter (μ)					
	0	0.1	0.2	0.3	0.4	0.5
Ke *et al.* (2015)	0.5453	0.5102	0.4352	0.3609	0.3011	0.2553
present	0.54663	0.511391	0.436224	0.361772	0.301781	0.25587

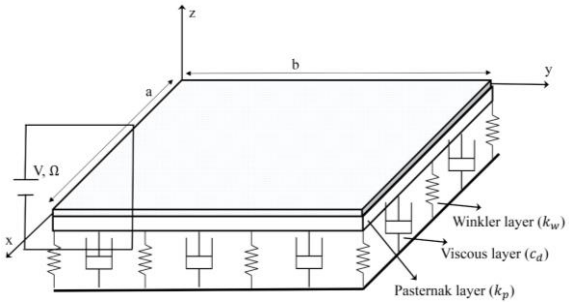

Fig. 1 Configuration of nanoplate resting on viscoelastic substrate

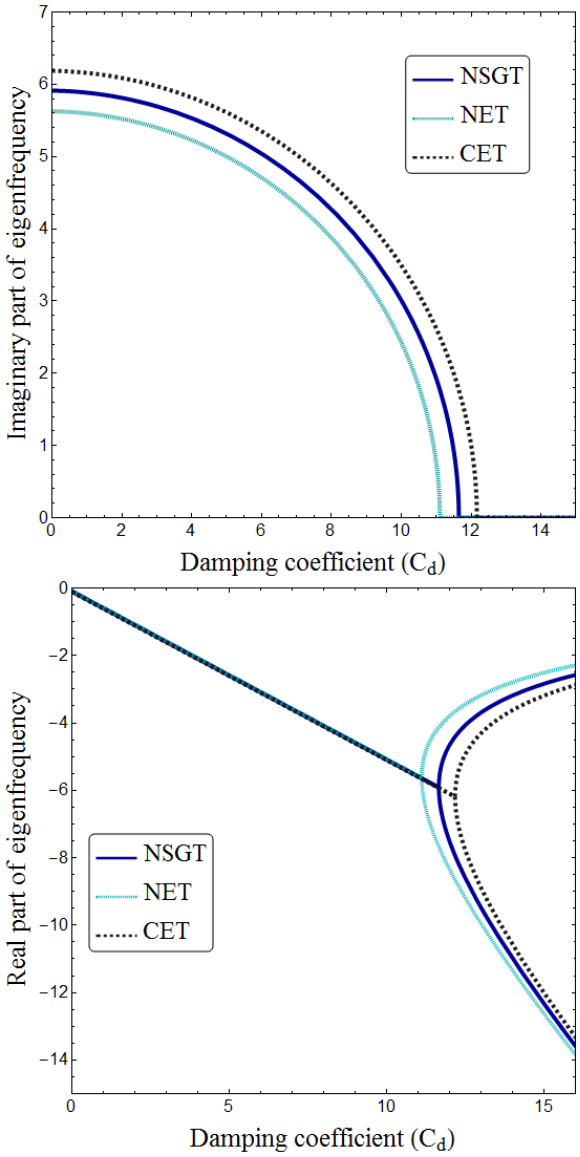

Fig. 2 Variation of real and imaginary parts of eigenfrequency versus damping coefficient for different elasticity theories (μ=2 nm^2, λ=1 nm^2, K_w=5, K_p=0.5, V=Ω=0, G_d=0.01).

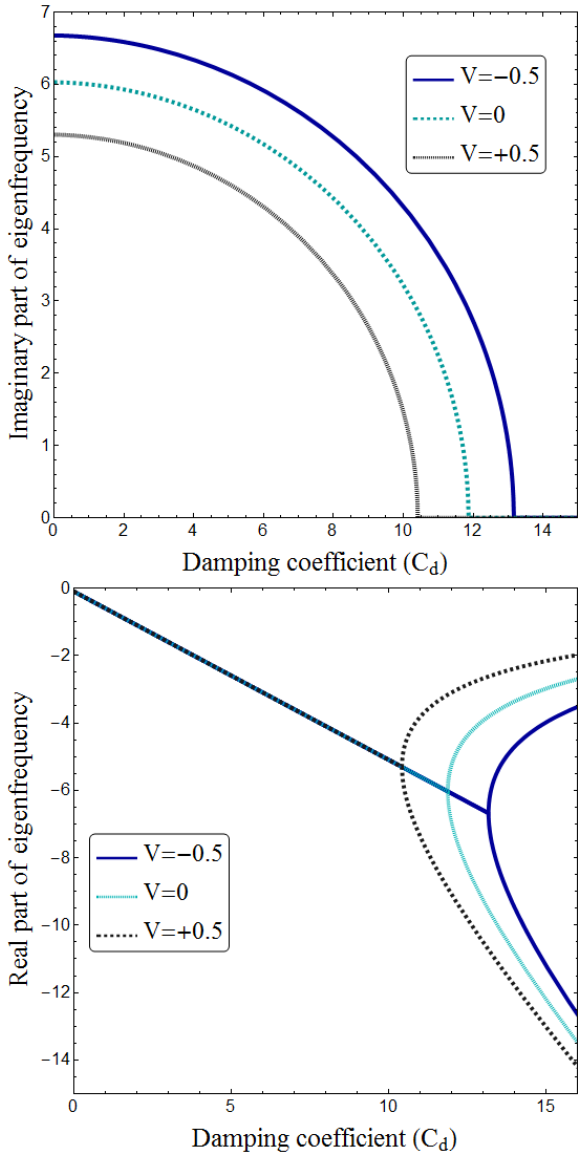

Fig. 3 Variation of real and imaginary parts of eigenfrequency versus damping coefficient for different electric voltages (μ=1 nm^2, λ=0.5 nm^2, K_w=5, K_p=0.5, G_d=0.01).

when K_w=5, K_p=0.5. When μ=0 and λ=0, the results based on classical continuum mechanics are rendered. It is observed that frequency of magneto-electro-viscoelastic nanoplate reduces by inclusion of nonlocal parameter. This observation indicates that nonlocal parameter exerts a stiffness-softening effect which leads to lower vibration frequencies. But, effect of nonlocal parameter on the magnitude of frequencies depends on the value of strain gradient or length scale parameter. In fact, frequency of nanoplate increases with increase of length scale parameter which highlights the stiffness-hardening effect due to the strain gradients. It should be pointed out that increase of damping coefficient degrades the plate stiffness and imaginary eigenfrequencies reduce until a critical point in which the frequencies become zero. At this point, the nanoplate is critically damped and does not oscillate. However, obtained critical damping coefficients (C_{cr}) depend on the value of length scale parameter. In fact, inclusion of length scale parameter in nonlocal strain gradient theory leads to higher critical damping coefficients compared with nonlocal theory. So, it can be concluded that critical damping coefficients obtained by nonlocal elasticity theory are underestimated. As a consequence, it is very important to consider both nonlocal and length scale parameters in analysis of smart nanoplates. However, real part of eigenfrequency is not affected by the nonlocal and strain gradient effects at small damping coefficients. But, effect of scale parameters on real part of eigenfrequency becomes important after the critical damping coefficient.

Effects of applied voltage and magnetic potential on damping vibration behavior of smart magneto-electro-viscoelastic nanoplates are respectively shown in Figs. 3 and 4 when μ=1 nm^2, λ=0.5 nm^2, K_w=5, K_p=0.5 and G_d=0.01. It is seen that magnitude and sign of applied

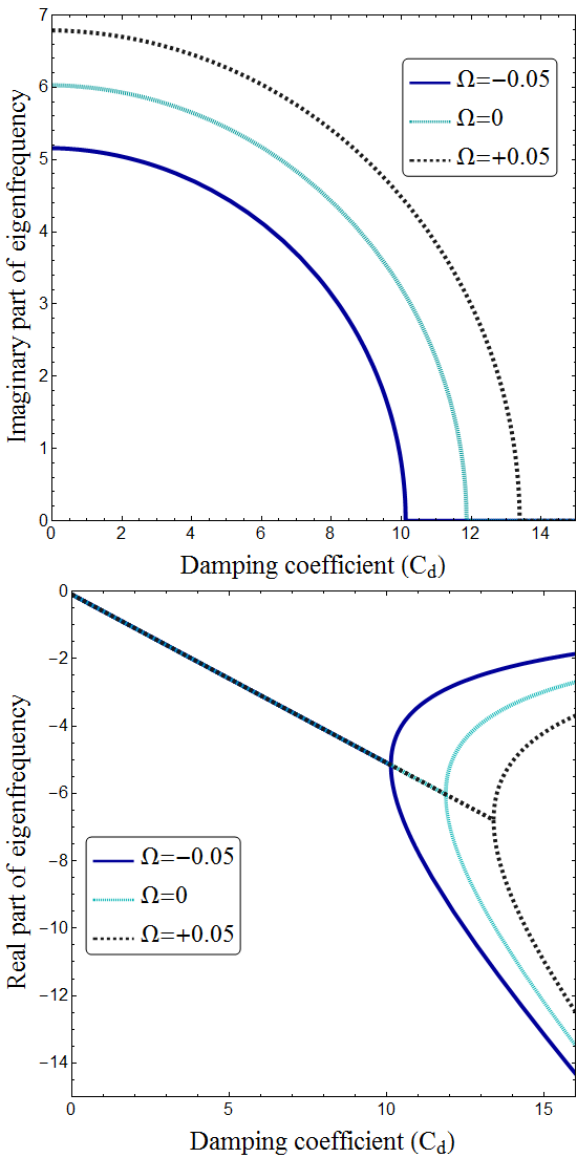

Fig. 4 Variation of real and imaginary parts of eigenfrequency versus damping coefficient for different magnetic potentials (μ=1 nm^2, λ=0.5 nm^2, K_w=5, K_p=0.5, G_d=0.01).

voltage and magnetic potential have a great effect on critical damping coefficients of nanoplates. In fact, negative voltages provide larger critical damping coefficients compared with positive voltages. In contrast, negative magnetic potentials give smaller critical damping coefficients. In other words, increasing magnetic potential from negative to positive values leads to enlargement of critical damping coefficients. This observations are due to the compressive and tensile loads exerted by electric and magnetic fields, respectively. So, vibration behavior of nanoplates can be controlled by exerting appropriate magnetic and electric fields to the nanoplate.

Fig. 5 presents the variation of imaginary part of eigenfrequency versus magnetic potential for different electric voltages and structural damping coefficients (G_d) at μ=1 nm^2, λ=0.5 nm^2, K_w=5, K_p=0.5, C_d=2. It is found that increase of structural damping coefficients leads to

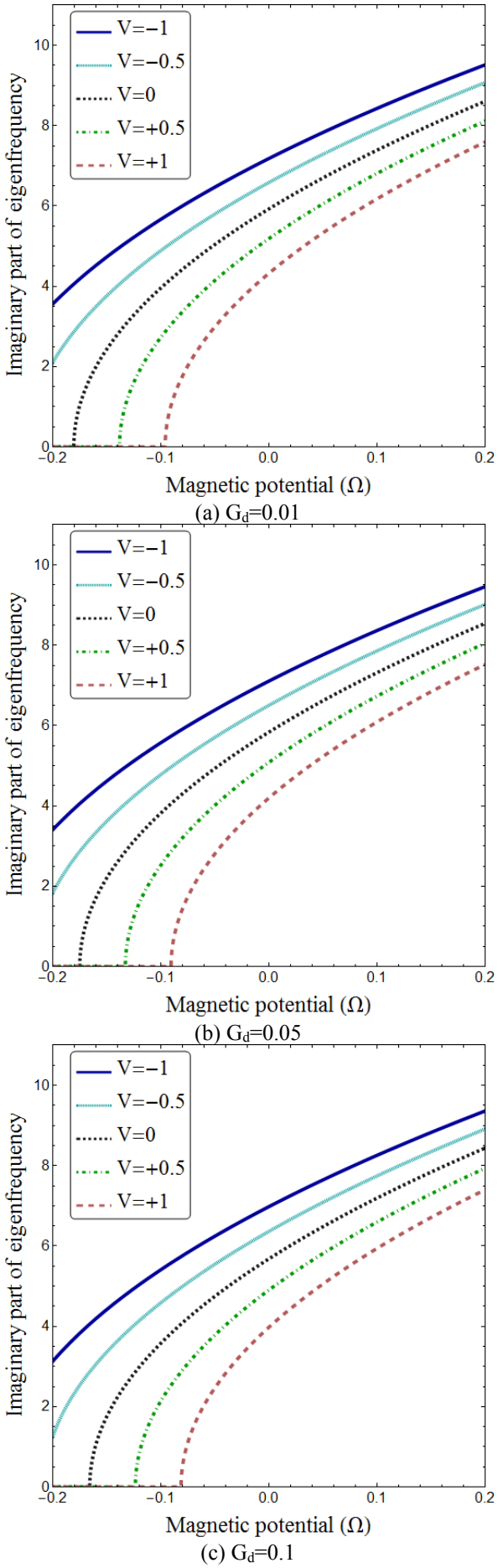

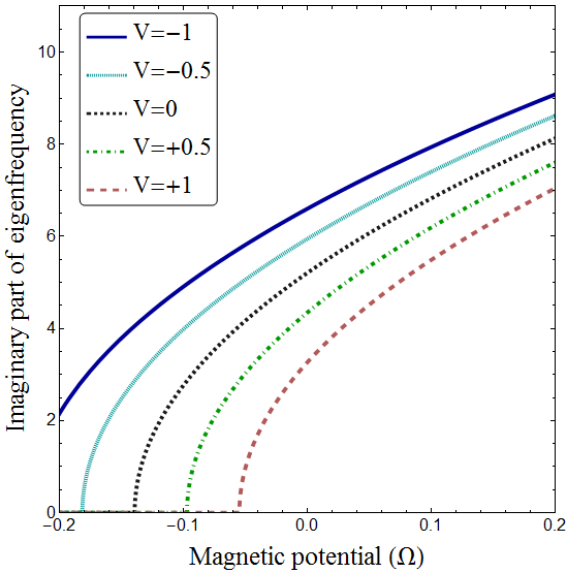

(d) G_d=0.2

Fig. 5 Variation of imaginary part of eigenfrequency versus magnetic potential for different electric voltages and structural damping coefficients (μ=1 nm^2, λ=0.5 nm^2, K_w=5, K_p=0.5, C_d=2)

vibration damping of nanoplate at small values of magnetic potential. For example, when V=-0.5, vibration of system is underdamped for G_d=0.01, 0.05 and 0.1. But, vibration of nanoplate becomes damped when V=-0.5 and G_d=0.2. However, by increasing in magnetic potential, vibration of nanoplate becomes undamped. In fact, higher values of magnetic potential lead to postponement in vibration damping of nanoplates.

In Fig.6, variation of imaginary part of eigenfrequency versus electric voltage for different Winkler and Pasternak parameters is plotted at μ=1 nm^2, λ=0.5 nm^2, G_d=0.01 and C_d=2. It is found that increase of applied voltage from negative to positive values may results in vibration damping on nanoplate. In fact, at a certain value of applied voltage the system becomes damped and does not oscillate. These observations are significantly affected by the values of Winkler and Pasternak parameters. In fact, Pasternak layer provides a continuous interaction with graphene sheet, while Winkler layer has a discontinuous interaction with the nanoplate. Increasing Winkler and Pasternak parameters leads to larger frequencies by enhancing the bending rigidity of nanoplates. But, Pasternak layer shows more increasing effect on the frequencies compared with Winkler layer. It is found that increasing foundation parameters yields larger critical voltages. In fact, higher values of foundation parameters lead to a significant delay in vibration damping of nanoplates.

Time response of nonlocal strain gradient nanoplates for different damping coefficients is plotted in Fig. 7 when μ=2 nm^2, λ=1 nm^2, K_w=5 and K_p=0.5. It is seen that with the time increment, amplitude of system reduces. This reduction in amplitude of system depends on the value of damping coefficient. As the value of damping coefficient increases, vibration of magneto-electro-viscoelastic nanoplate becomes damped with higher rates. At larger damping coefficients, vibration of nanoplate is damped after a few number of oscillation.

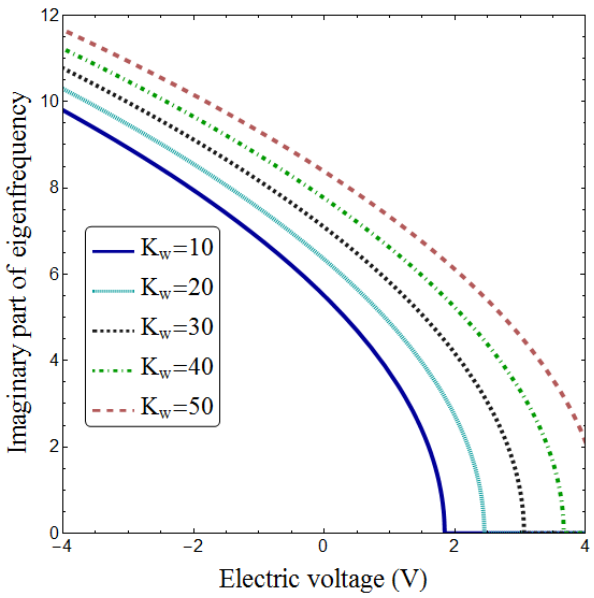

(a) K_p=0

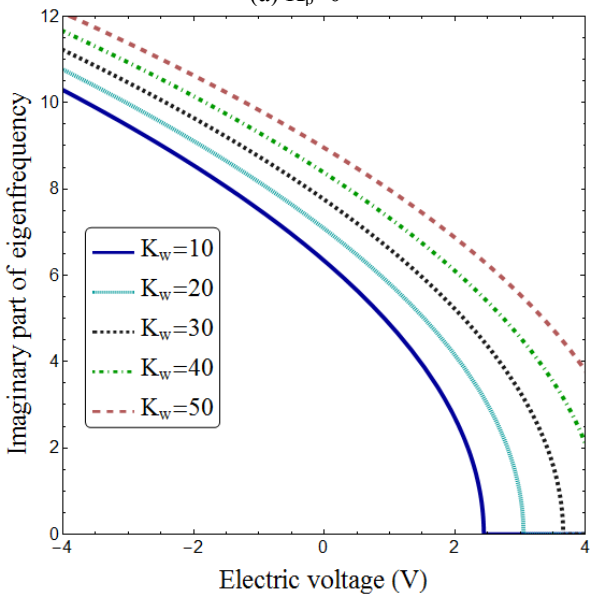

(b) K_p=0.5

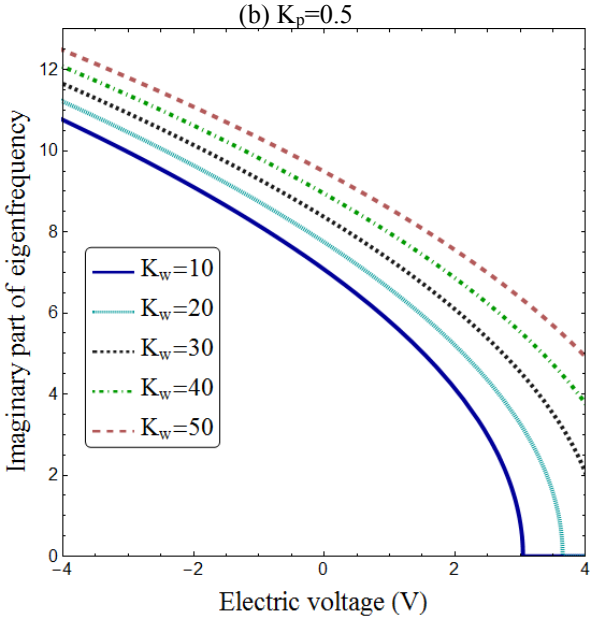

(c) K_p=1

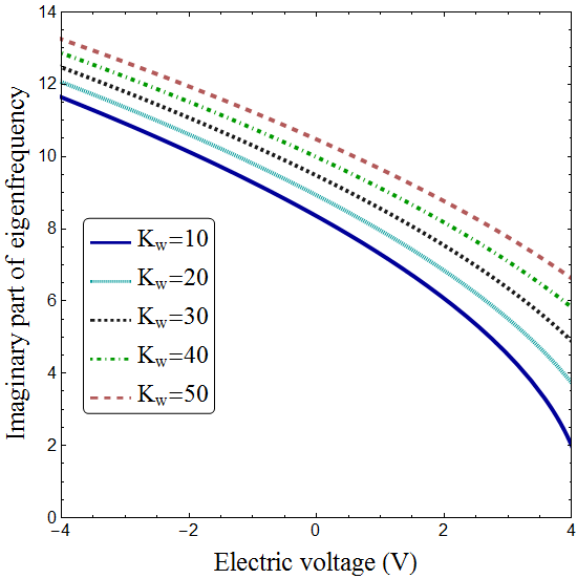

(d) K_p=2

Fig. 6 Variation of imaginary part of eigenfrequency versus electric voltage for different Winkler and Pasternak parameters (μ=1 nm^2, λ=0.5 nm^2, G_d=0.01, C_d=2)

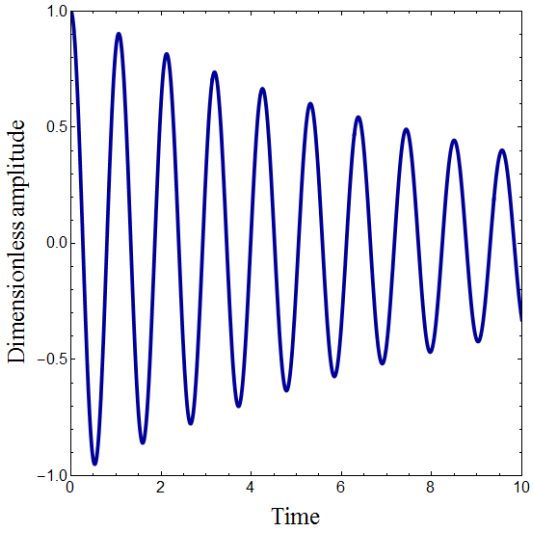

(a) C_d=0

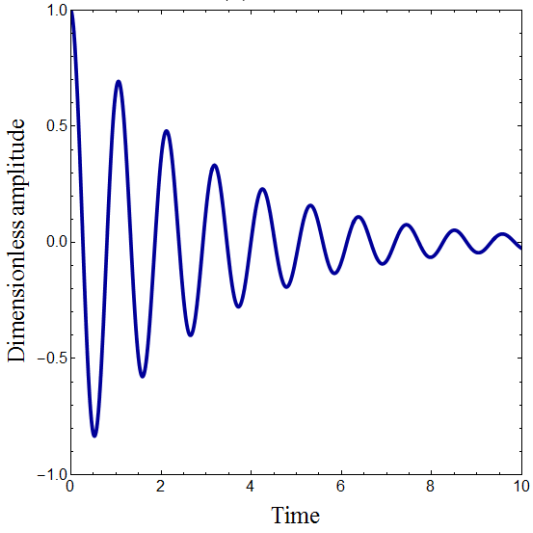

(b) C_d=0.5

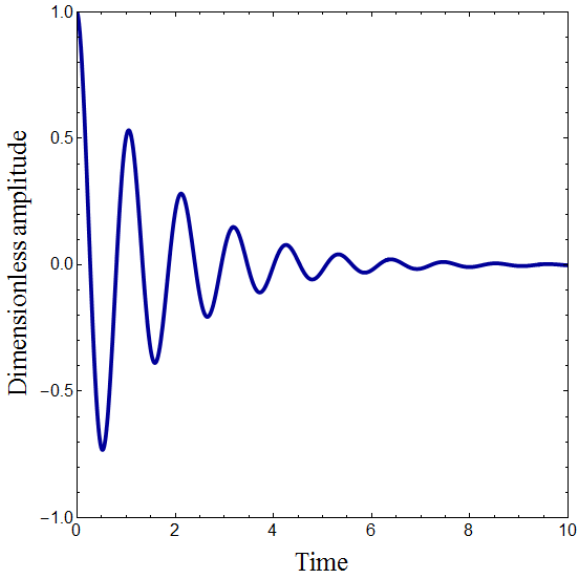

(c) C_d=1

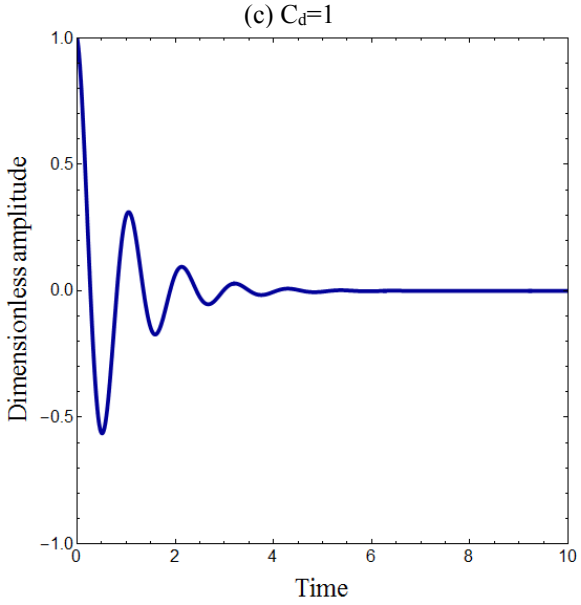

(d) C_d=2

Fig. 7 Time response of nonlocal strain gradient MEE nanoplate for different damping coefficients (μ=2 nm^2, λ=1 nm^2, K_w=5, K_p=0.5, G_d=0.01)

5. Conclusions

In this paper, nonlocal strain gradient theory is employed to investigate damping vibration behavior of magneto-electro-viscoelastic nanoplates resting on viscoelastic medium. The theory introduces two scale parameters corresponding to nonlocal and strain gradient effects to capture both stiffness-softening and stiffness-hardening influences. Hamilton's principle is employed to obtain the governing equation of a nonlocal strain gradient nanoplate. These equations are solved via Galerkin's method to obtain the frequencies. It is observed that frequency of nanoplate reduces with increase of nonlocal parameter. In contrast, frequency increases with increase of length scale parameter which highlights the stiffness-hardening effect due to the strain gradients. Also, increase

of damping coefficient degrades the plate stiffness and vibration frequencies reduce until a critical point in which the frequencies become zero. It is seen that nonlocal strain gradient theory provides larger critical damping coefficient than nonlocal elasticity theory. In fact, considering strain gradient effects leads to postponement is damping of smart nanoplates. All these observations are affected by the magnetic and electrical loading which enhances/decreases the plate stiffness and increases/ decreases the critical damping coefficient.

References

Aksencer, T. and Aydogdu, M. (2011), "Levy type solution method for vibration and buckling of nanoplates using nonlocal elasticity theory", *Physica E*, **43**(4), 954-959. https://doi.org/10.1016/j.physe.2010.11.024.

Ansari, R. and Gholami, R. (2016), "Nonlocal free vibration in the pre-and post-buckled states of magneto-electro-thermo elastic rectangular nanoplates with various edge conditions", *Smart Mater. Struct.*, **25**(9). https://doi.org/10.1088/0964-1726/25/9/095033.

Ansari, R. and Sahmani, S. (2013), "Prediction of biaxial buckling behavior of single-layered graphene sheets based on nonlocal plate models and molecular dynamics simulations", *Appl. Math. Model.*, **37**(12), 7338-7351. https://doi.org/10.1016/j.apm.2013.03.004.

Ansari, R., Arash, B. and Rouhi, H. (2011), "Vibration characteristics of embedded multi-layered graphene sheets with different boundary conditions via nonlocal elasticity", *Compos. Struct.*, **93**(9), 2419-2429. https://doi.org/10.1016/j.compstruct.2011.04.006.

Arani, A.G., Haghparast, E. and Zarei, H.B. (2016), "Nonlocal vibration of axially moving graphene sheet resting on orthotropic visco-Pasternak foundation under longitudinal magnetic field", *Physica B*, **495**, 35-49. https://doi.org/10.1016/j.physb.2016.04.039.

Bessaim, A., Houari, M.S.A., Bernard, F. and Tounsi, A. (2015), "A nonlocal quasi-3D trigonometric plate model for free vibration behaviour of micro/nanoscale plates", *Struct. Eng. Mech.*, **56**(2), 223-240. https://doi.org/10.12989/sem.2015.56.2.223.

Ebrahimi, F. and Barati, M.R. (2016a), "Vibration analysis of nonlocal beams made of functionally graded material in thermal environment", *Europ. Phys. J. Plus*, **131**(8), 279. https://doi.org/10.1140/epjp/i2016-16279-y.

Ebrahimi, F. and Barati, M.R. (2016b), "A unified formulation for dynamic analysis of nonlocal heterogeneous nanobeams in hygro-thermal environment", *Appl. Phys. A.*, **122**(9), 792. https://doi.org/10.1007/s00339-016-0322-2.

Ebrahimi, F. and Barati, M.R. (2016c), "A nonlocal higher-order refined magneto-electro-viscoelastic beam model for dynamic analysis of smart nanostructures", *J. Eng. Sci.*, **107**, 183-196. https://doi.org/10.1016/j.ijengsci.2016.08.001.

Ebrahimi, F. and Barati, M.R. (2016d), "Hygrothermal buckling analysis of magnetically actuated embedded higher order functionally graded nanoscale beams considering the neutral surface position", *J. Therm. Stress*, **39**(10), 1210-1229. https://doi.org/10.1080/01495739.2016.1215726.

Ebrahimi, F. and Barati, M.R. (2016e), "Vibration analysis of smart piezoelectrically actuated nanobeams subjected to magneto-electrical field in thermal environment", *J. Vib. Control*, **24**(3), 549-564. https://doi.org/10.1177/1077546316646239.

Ebrahimi, F. and Barati, M.R. (2016f), "Static stability analysis of smart magneto-electro-elastic heterogeneous nanoplates embedded in an elastic medium based on a four-variable refined plate theory", *Smart Mater. Struct.*, **25**(10), https://doi.org/10.1088/0964-1726/25/10/105014

Ebrahimi, F. and Barati, M.R. (2016g), "Wave propagation analysis of quasi-3D FG nanobeams in thermal environment based on nonlocal strain gradient theory", *Appl. Phys. A.*, **122(**9), 843. https://doi.org/10.1007/s00339-016-0368-1.

Ebrahimi, F. and Barati, M.R. (2016h), "Size-dependent dynamic modeling of inhomogeneous curved nanobeams embedded in elastic medium based on nonlocal strain gradient theory", *Proceedings of the Institution of Mechanical Engineers, Part C: Journal of Mechanical Engineering Science*, **231**(23), 4457-4469. https://doi.org/10.1177/0954406216668912.

Ebrahimi, F. and Barati, M.R. (2017i), "Hygrothermal effects on vibration characteristics of viscoelastic FG nanobeams based on nonlocal strain gradient theory", *Compos. Struct.*, **159**, 433-444. https://doi.org/10.1016/j.compstruct.2016.09.092.

Ebrahimi, F. and Barati, M.R. (2017j), "A nonlocal strain gradient refined beam model for buckling analysis of size-dependent shear-deformable curved FG nanobeams", *Compos. Struct.*, **159,** 174-182. https://doi.org/10.1016/j.compstruct.2016.09.058.

Ebrahimi, F. and Salari, E. (2015), "Thermo-mechanical vibration analysis of a single-walled carbon nanotube embedded in an elastic medium based on higher-order shear deformation beam theory", *J. Mech. Sci. Technol.*, **29**(9), 3797-3803. https://doi.org/10.1007/s12206-015-0826-2.

Ebrahimi, F., Barati, M.R. and Dabbagh, A. (2016), "A nonlocal strain gradient theory for wave propagation analysis in temperature-dependent inhomogeneous nanoplates", *J. Eng. Sci.*, **107,** 169-182. https://doi.org/10.1016/j.ijengsci.2016.07.008.

Eringen, A.C. (1983), "On differential equations of nonlocal elasticity and solutions of screw dislocation and surface waves", *J. Appl. Phys.*, **54**(9), 4703-4710. https://doi.org/10.1063/1.332803.

Eringen, A.C. and Edelen, D.G.B. (1972), "On nonlocal elasticity", *J. Eng. Sci.*, **10**(3), 233-248. https://doi.org/10.1016/0020-7225(72)90039-0.

Farajpour, A., Shahidi, A.R., Mohammadi, M. and Mahzoon, M. (2012), "Buckling of orthotropic micro/nanoscale plates under linearly varying in-plane load via nonlocal continuum mechanics", *Compos. Struct.*, **94**(5), 1605-1615. https://doi.org/10.1016/j.compstruct.2011.12.032.

Farajpour, A., Yazdi, M.H., Rastgoo, A., Loghmani, M. and Mohammadi, M. (2016), "Nonlocal nonlinear plate model for large amplitude vibration of magneto-electro-elastic nanoplates", *Compos. Struct.*, **140**, 323-336. https://doi.org/10.1016/j.compstruct.2015.12.039.

Hashemi, S.H., Mehrabani, H. and Ahmadi-Savadkoohi, A. (2015), "Exact solution for free vibration of coupled double viscoelastic graphene sheets by visco Pasternak medium", *Compos. Part B*, **78**, 377-383. https://doi.org/10.1016/j.compositesb.2015.04.008.

Ke, L.L., Liu, C. and Wang, Y.S. (2015), "Free vibration of nonlocal piezoelectric nanoplates under various boundary conditions", *Physica E*, **66**, 93-106. https://doi.org/10.1016/j.physe.2014.10.002.

Lam, D.C.C., Yang, F., Chong, A.C.M., Wang, J. and Tong, P. (2003), "Experiments and theory in strain gradient elasticity", *J. Mech. Phys. Solid*, **51**(8), 1477-1508. https://doi.org/10.1016/S0022-5096(03)00053-X.

Li, L. and Hu, Y. (2016), "Wave propagation in fluid-conveying viscoelastic carbon nanotubes based on nonlocal strain gradient theory", *Comput. Mater. Sci.*, **112,** 282-288. https://doi.org/10.1016/j.commatsci.2015.10.044.

Li, L., Hu, Y. and Li, X. (2016), "Longitudinal vibration of size-dependent rods via nonlocal strain gradient theory", *J. Mech. Sci.*, **115**, 135-144. https://doi.org/10.1016/j.ijmecsci.2016.06.011.

Li, Y.S., Cai, Z.Y. and Shi, S.Y. (2014), "Buckling and free

vibration of magnetoelectroelastic nanoplate based on nonlocal theory", *Compos. Struct.*, **111**, 522-529. https://doi.org/10.1016/j.compstruct.2014.01.033.

Lim, C.W., Zhang, G. and Reddy, J.N. (2015), "A higher-order nonlocal elasticity and strain gradient theory and its applications in wave propagation", *J. Mech. Phys. Solid*, **78,** 298-313. https://doi.org/10.1016/j.jmps.2015.02.001.

Mohammadi, M., Farajpour, A., Moradi, A. and Ghayour, M. (2014), "Shear buckling of orthotropic rectangular graphene sheet embedded in an elastic medium in thermal environment", *Compos. Part B*, **56**, 629-637. https://doi.org/10.1016/j.compositesb.2013.08.060.

Mohammadi, M., Goodarzi, M., Ghayour, M. and Farajpour, A. (2013), "Influence of in-plane pre-load on the vibration frequency of circular graphene sheet via nonlocal continuum theory", *Compos. Part B*, **51**, 121-129. https://doi.org/10.1016/j.compositesb.2013.02.044.

Murmu, T., McCarthy, M.A. and Adhikari, S. (2013), "In-plane magnetic field affected transverse vibration of embedded single-layer graphene sheets using equivalent nonlocal elasticity approach", *Compos. Struct.*, **96**, 57-63. https://doi.org/10.1016/j.compstruct.2012.09.005.

Pradhan, S. C. and Murmu, T. (2009), "Small scale effect on the buckling of single-layered graphene sheets under biaxial compression via nonlocal continuum mechanics", *Comput. Mater. Sci.*, **47**(1), 268-274. https://doi.org/10.1016/j.commatsci.2009.08.001.

Pradhan, S.C. and Kumar, A. (2011), "Vibration analysis of orthotropic graphene sheets using nonlocal elasticity theory and differential quadrature method", *Compos. Struct.*, **93**(2), 774-779. https://doi.org/10.1016/j.compstruct.2010.08.004.

Shen, Z.B., Tang, H.L., Li, D.K. and Tang, G.J. (2012), "Vibration of single-layered graphene sheet-based nanomechanical sensor via nonlocal Kirchhoff plate theory", *Comput. Mater. Sci.*, **61**, 200-205. https://doi.org/10.1016/j.commatsci.2012.04.003.

Zenkour, A.M. (2016), "Nonlocal transient thermal analysis of a single-layered graphene sheet embedded in viscoelastic medium", *Physica E*, **79**, 87-97. https://doi.org/10.1016/j.physe.2015.12.003.

PL